ANALIZA VITKIH RAZPOKANIH NOSILCEV NA WINKLERJEVI ZEMLJINI Z UPORABO POENOSTAVLJENEGA RAČUNSKEGA MODELA

MATJAŽ SKRINAR IN BORIS LUTAR

o avtorjih

Matjaž Skrinar
University of Maribor,
Faculty of Civil Engineering
Smetanova 17, 2000 Maribor, Slovenija
E-pošta: skrinar@uni-mb.si

Boris Lutar
University of Maribor,
Faculty of Civil Engineering
Smetanova 17, 2000 Maribor, Slovenija
E-pošta: lutar@uni-mb.si

izvleček

Članek obravnava uporabo pogosto uporabljenega poenostavljenega računskega modela za analitični izračun prečnih premikov vitkih nosilcev, vgrajenih v Winklerjevi zemljini, ki so prečno razpokani. Prikazano je reševanje pripadajočih diferencialnih enačb in pridobitev natančnih analitičnih rešitev za izračun prečnih premikov poenostavljenega modela. Rešitve za pomike omogočajo izračun porazdelitve notranjih upogibnih momentov in strižnih sil z uporabo znanih zvez iz Euler-Bernoullijeve teorije upogiba ali z uporabo dveh mehanskih ravnotežnih pogojev.

Numerična primera pokrivata obtežni situaciji, na kratko predstavljata možnosti uporabe modela in potrjujeta uporabnost predstavljenega pristopa. Rezultati, ki so pridobljeni s predstavljenim pristopom, so primerjani še z vrednostmi iz obsežnih diskretnih računskih modelov po metodi končnih elementov, tvorjenimi z 2D končnimi elementi. Očitno je, da se velike razlike obsega vloženega računskega dela modelov ne odražajo v pomembnih razlikah rezultatov med računskima modeloma.

ključne besede

nosilci s prečnimi razpokami, poenostavljeni računski model, elastična podlaga, Winklerjeva zemljina, prečni pomiki, upogibni momenti in prečne sile

ANALYSIS OF CRACKED SLENDER-BEAMS ON WINKLER'S FOUNDATION USING A SIMPLIFIED COMPUTATIONAL MODEL

MATJAŽ SKRINAR and BORIS LUTAR

about the authors

Matjaž Skrinar
University of Maribor,
Faculty of Civil Engineering
Smetanova 17, 2000 Maribor, Slovenia
E-mail: skrinar@uni-mb.si

Boris Lutar
University of Maribor,
Faculty of Civil Engineering
Smetanova 17, 2000 Maribor, Slovenia
E-mail: lutar@uni-mb.si

Abstract

This paper discusses the coupling of Winkler's soil model with a simplified computational model that is widely used for the calculation of transverse displacements in transversely cracked slender beams. The bending problem of a cracked beam embedded in Winkler's soil is addressed by means of an analytical approach. The solving of the corresponding differential equation solutions is studied in order to obtain exact analytical expressions for the transverse displacements of the simplified computational model. After the solutions for the displacements of the beam are obtained, the inner bending moment and the shear force distributions within the beam can be calculated, either by using known, established relationships from the Euler–Bernoulli beam theory or by implementing two mechanical equilibrium conditions.

Numerical examples covering several load situations are briefly presented in order to support the discussed approach. The results obtained with the presented approach are then further compared with the values from huge 2D finite-element models, where a detailed description of the crack was achieved using the discrete approach. It is evident that any drastic difference in the computational effort is not reflected in the significant differences in the results between the models.

keywords

beams with transverse cracks, simplified computational model, elastic foundation, Winkler's soil, transverse displacements, bending moment and shear forces

1 INTRODUCTION

Although cracks can certainly be considered as one of the most unfavourable effects that might occur in a structure, and many efforts are invested in their prevention during the utilization of a structure, some engineering situations actually require their inclusion within the analysis. A typical example of such a situation is in the design of structures for earthquake resistance, according to the current regulations. The EN 1998 standard, for example, requires that in concrete buildings, in composite steel-concrete buildings, and in masonry buildings, the stiffness of the load-bearing elements should, in general, be evaluated by taking into account the effect of cracking. This standard further allows for the two elastic (flexural as well as shear, but not axial) stiffness properties of concrete and masonry elements to be taken as being equal to one half of the corresponding stiffness of the non-cracked elements, unless a more accurate analysis of the cracked elements is performed. Since the explicit modelling of cracks requires the implementation 2D or 3D finite elements, where a detailed discretisation of the crack and its surrounding can be properly achieved with an appropriate mesh of finite elements, an accurate analysis is time-consuming and demands a substantial computational effort.

However, the structural analysis of cracked beams is of great engineering interest (although primarily from the inverse-identification point of view), and has been extensively studied over recent decades, resulting in numerous investigations. Several studies have confirmed that cracks can be successfully and implicitly treated as slope discontinuities within a 1D model of a beam. This simplified model, given by Okamura et al. [1], where

the crack is represented by means of an internal hinge endowed with a massless rotational spring (using the linear moment-rotation constitutive law), thus connecting those non-cracked parts of the structure that are modelled as elastic elements, represents the basis for a number of papers. Okamura et al. further introduced the earliest definition for the rotational linear spring stiffness Kr of a rectangular cross-section. In addition, some other researchers [2-8] have presented their definitions.

The model was successfully implemented for a direct analysis of the dynamics when determining the natural frequencies and mode shapes (Shifrin and Ruotolo [9], Khiem and Lien [10], Li [11], Fernández-Sáez and Navarro [12]).

Okamura's simplified computational model has already been implemented regarding the experimental inverse identification of a crack (Rizos et al. [13], Boltežar et al. [14], Vestroni and Capecchi [15], Bamnios et al. [16]).

However, since the governing differential equations of a bending displacement can only be solved analytically for moderate structures, the research interest has further oriented towards finite-element solutions (Gounaris and Dimarogonas [17], Skrinar and Umek [18], Skrinar [19], Krawczuk and Žak [20], Kisa and Brandon [21]).

Two main approaches exist for the modelling of cracks within those derivations based on the same computational model. Although they converge towards the same results, they differ regarding genuine mechanical descriptions, and also mathematical instrumentations. The first approach, also implemented within the presented manuscript, appears to be more mechanical (or engineering). It is based on the solutions of coupled governing differential equations for the elastic non-cracked regions where the cracks are modelled as slope discontinuities ([7], [9], [10], [12], [14], [16], [18], [19], [20], [22]). For various types of problems, the general solutions (as functions of four integration constants only) are usually given in advance, and the influence of the cracks is hence taken into account regarding four continuity conditions at each location. Consequently, the coefficients that govern displacement functions are explicit functions of pure mechanical information – the stiffnesses of rotational springs. In the second approach, the singularities of flexural stiffness, as represented by the Dirac delta unit step functions, are directly introduced within the governing differential equation (Caddemi and Caliò [23], Biondi and Caddemi [24,25]). This governing equation is, thus, exclusively formulated over the entire domain of the beam without the explicit enforcement of any of those continuity conditions already accounted for in the adopted flexural stiffness model. However, in order to prevent meaningless negative values for either the flexural rigidity or the rotational stiffness, as caused by the negative impulses applied to the flexural rigidity of the element, those coefficients (without any apparent physical interpretation) that govern the solution of a unique governing differential equation, must additionally fulfil certain mathematical conditions.

In order to expand previous realizations, the scope of the presented paper is oriented towards an examination of the simplified model's behaviour regarding the problems of slender-cracked beams resting on an elastic soil. The idea of modelling soil as an elastic medium was first introduced by Winkler, and since then Winkler's soil model has been the focus of extensive research. This model is the most convenient representation of soil support within the domain of linear elasticity for framed structure-soil interaction analyses. Several approaches to the analysis of non-cracked beams on elastic foundations can be found in the literature. Jones [26] implemented a finite difference theory, Chen [27] used differential quadrature to discretize the governing differential equations defined on all elements for solving the problem of beams resting on an elastic foundation, Onu [28] derived a formulation leading to an explicit free-of meshing stiffness matrix for a beam finite-element foundation model. Guo and Weitsman [29] employed Green's foundation formulation to evaluate the response of beams on non-uniform elastic foundations, with the nonlinear material and geometric behaviours of reinforced concrete. The non-linear material and geometric behaviour of reinforced concrete deep-beams resting on a linear or non-linear Winkler's foundation was studied by Al-Azzawi et al. [30], by implementing a smeared-crack model within a finite-elements model established with ANSYS computer software. For a solution using a layer finite-element method, an incremental approach within a modified Newton-Raphson iteration method was employed by Cerioni and Mingardi [31]. The design analysis of beams, circular plates, and cylindrical tanks, on elastic foundations with a beam/strip analysis, was also studied by Melerski [32].

This paper studies those analytical equations for the load-displacement response of a cracked-elastic beam on a Winkler's soil model, as established through the solutions from governing differential equations, regarding an implemented, simplified crack-model. These solutions can be established in a straightforward manner, in order to yield a system of linear algebraic equations that can be solved by elementary numerical techniques. To complete the study, the results obtained with the simplified computational model are compared with the results obtained from more precise, as well as detailed and,

consequently, more computational effort requiring large 2D finite elements models where the discrete approach is utilized for the description of the crack. The presented examples confirm that the elaborated solutions may be effectively implemented for static structural analyses, where cracked beam-like elements are required.

2 SIMPLIFIED MODEL FOR CRACKED BEAMS ON WINKLER'S FOUNDATION

One of the simplest models for a mathematical description of a cracked structure's response behaviour is a model where the crack is introduced as a rotational linear spring connecting the non-cracked parts of the structure, as presented by Okamura et al. [1] (Fig. 1). Due to the localized effect of the crack, both the non-cracked adjacent parts of the element (to the left and to the right of the crack) are modelled as elastic sections.

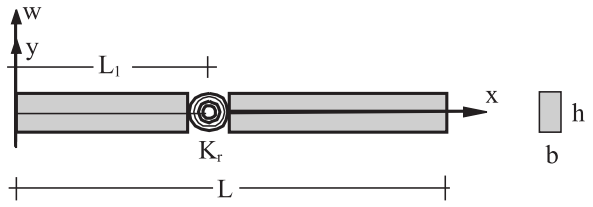

Figure 1. Okamura's computational model for transverse displacements.

The crack is defined by its location (i.e., the distance L_1 from the left-hand end), and depth d. The transverse displacements are thus (in addition to all the other parameters of the structure) a function of the crack stiffness K_r. The stiffness of the massless rotational spring depends on the height of the non-cracked cross-section h, the relative depth of the crack $\delta=d/h$, and the product of the Young's modulus E with the moment of inertia of the non-cracked cross-section I, i.e., the flexural rigidity EI. Okamura et al. introduced the earliest definition of rotational stiffness, and this is the only definition that also takes Poisson's ratio ν into account:

$$\mathrm{K_r} = \frac{EI}{h \cdot 6 \cdot (1-\nu^2) \cdot F(\delta)} \qquad (1)$$

with

$$F(\delta) = 1.98 \cdot \delta^2 - 3.277 \cdot \delta^3 + 14.43 \cdot \delta^4 - 31.26 \cdot \delta^5 + 63.56 \cdot \delta^6 - 103.36 \cdot \delta^7 + 147.52 \cdot \delta^8 - 127.69 \cdot \delta^9 + 61.50 \cdot \delta^{10}$$

When studying the elastic displacement of a non-cracked beam element of infinitesimal length, it is possible to derive a governing differential equation that relates to the coordinate x, transverse displacement $w(x)$, the geometrical and mechanical properties of the cross-section (flexural rigidity EI), and the applied transverse load $q(x)$. The general solution of the equation for a beam on Winkler's soil model, which is a fourth-order ordinary differential equation with constant coefficients, can be given in two alternative mathematical forms. The form, as used in this manuscript, can be found in many structural textbooks, for example, in Oden, [33]:

$$w(x) = e^{\beta \cdot x} \cdot \left(A \cdot \cos(\beta \cdot x) + B \cdot \sin(\beta \cdot x)\right) + e^{-\beta \cdot x} \cdot \left(C \cdot \cos(\beta \cdot x) + D \cdot \sin(\beta \cdot x)\right) + \text{particular integral} \qquad (2)$$

with

$$\beta = \sqrt[4]{\frac{k}{4 \cdot E \cdot I}}$$

where A, B, C and D are constants of the integration obtained from boundary conditions, whilst the particular integral depends on the mathematical form of the load $q(x)$. The constant k is referred to as the constant of proportionality, given as a product of the modulus (or coefficient) of the subgrade reaction k_s with the width of the beam b. The relationship between the soil subgrade reaction modulus and its elastic properties, i.e., the modulus of elasticity for the elastic medium E_f and the Poisson's ratio ν_f is given by a formula developed by Selvadurai [34]:

$$k_s = \frac{0.65 \cdot E_f}{b \cdot \left(1-\nu_f^2\right)}$$

However, since the crack separates the beam into two elastic parts, the transverse displacements cannot be described by a single function anymore and, therefore, two displacement functions are required. Consequently, two coupled differential equations for the parts on the left- ($v_1(x)$) and right-hand ($v_2(x)$) sides of the crack, with eight unknown constants altogether, have to be solved simultaneously. The solutions, i.e., the functions $w_1(x)$ and $w_2(x)$ for the parts to the left and the right, respectively, implement eight unknown constants altogether:

$$w_1(x) = e^{\beta \cdot x} \cdot \left(A_1 \cdot \cos(\beta \cdot x) + B_1 \cdot \sin(\beta \cdot x)\right) + e^{-\beta \cdot x} \cdot \left(C_1 \cdot \cos(\beta \cdot x) + D_1 \cdot \sin(\beta \cdot x)\right) + \text{particular integral} \qquad (3)$$

$$w_2(x) = e^{\beta \cdot x} \cdot \left(A_2 \cdot \cos(\beta \cdot x) + B_2 \cdot \sin(\beta \cdot x)\right) + e^{-\beta \cdot x} \cdot \left(C_2 \cdot \cos(\beta \cdot x) + D_2 \cdot \sin(\beta \cdot x)\right) + \text{particular integral} \qquad (4)$$

Four of them are determined from the actual boundary conditions, and the remaining four are obtained from the continuity conditions at the crack location ($x=L_1$), where the influence of the crack is introduced as a slope discontinuity. These conditions are the equality of displacement:

$$w_1(L_1) = w_2(L_1), \qquad (5)$$

the condition for the discrete increase of the rotations:

$$\varphi_1(L_1) + \frac{EI \cdot w_1''(L_1)}{K_r} = \varphi_2(L_1), \qquad (6)$$

the equality of the bending moments:

$$w_1''(L_1) = w_2''(L_1), \qquad (7)$$

and the equality of the shear forces:

$$w_1'''(L_1) = w_2'''(L_1). \qquad (8)$$

The described approach can be straightforwardly expanded to cover a situation with N_c cracks that split the beam into N_{c+1} elastic segments. A transverse displacement computation requires solving the N_{c+1} coupled governing differential equations by implementing four mechanical boundary conditions and $4 \cdot N_c$ continuity conditions.

After the solutions for the displacements of the beam are obtained, the bending moment and shear force distributions within the beam can be calculated using the well-known relationships from the Euler–Bernoulli beam theory. However, with known solutions for the displacements, the problem becomes statically determinate. Consequently, the internal load distributions may also be fully determined by implementing two mechanical equilibrium conditions without using stiffness criteria.

The discussed approach even allows for analytical solutions of the transverse displacements to be constructed for some load situations. However, for two main reasons these solutions are not actually essential in engineering practice. Firstly, analytical solutions cannot cover all the general load cases that may appear, and furthermore, their derivations are also very time consuming. Secondly, in engineering practice, numerical results are sufficient for the analysis.

3 VALIDATIONS

Two load situations of a cracked structure were analyzed in order to verify the discussed approach. The length L of the beam was 10 m, the cross-section was a rectangle with dimensions of 0.80 m by 0.80 m, and the Young modulus was 33 GPa (corresponding to concrete grade C30/37). Two cracks were introduced at distances of 3 m and 2 m from the left- and right-hand ends, respectively. The depths of both cracks were 0.4 m and, from among all the existing definitions for a rotational spring, the definition given by Okamura was selected (producing the value $K_r = 4.423902 \cdot 10^8$ Nm) due to the fact that this is the only one that takes the Poisson's ratio into account. For this relative depth and a Poisson's ratio of 0.3, Okamura's definition produces results that have been proved to be in good agreement with those experimentally obtained values, as presented by Vestroni [35].

The Winkler's foundation was assumed to have a subgrade reaction modulus of k_s = 50 MPa/m.

Transverse displacements, shear forces, and bending moments along the structure's length were studied for all load cases.

The considered structure was furthermore modelled using finite elements by implementing the SolidWorks Simulation Professional v. 2011 finite-element program, where the discrete-crack approach was utilized to model the cracks. The transverse displacements and reactions were obtained from a computational model consisting of 163,369 2D six-noded quadrilateral second-order triangular-shell finite elements with more than 327,747 nodal points. In each node, three degrees of freedom were taken into account – vertical and horizontal displacements, as well as rotation. The vertical and horizontal displacements for each load combination were obtained in discrete points by solving approximately 2,000,000 linear equations.

3.1 LOAD CASE 1: THREE CONCENTRATED DOWNWARD FORCES

During the first load situation three vertical downward transverse forces were applied, located at the left-end (F_1=500 kN), mid-span (F_2=800 kN), and the right-end (F_3=250 kN), Fig. 2. Since the structure had two cracks and a concentrated in-field transverse load, the corresponding computational model of the considered load combination consisted of four elastic segments. Consequently, four coupled functions for four elastic regions had to be analyzed in order to obtain vertical displacement distributions along the structure. The interpolation functions for each region followed the mathematical form of Eq.(1), without a particular integral, since no distributed load was applied to the structure.

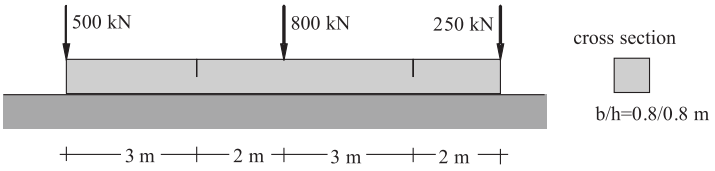

Figure 2. First example setup.

3.2 LOAD CASE 1: RESULTS AND DISCUSSION

The following functions for transverse displacements of the axis were obtained from the system of 16 linear algebraic equations (resulting from four coupled governing differential equations, GDE), by the implementation of mechanical boundary conditions, as well as continuity conditions:

$$w_1(x) = e^{-0.306957\cdot x}\cdot\left(\left(-7.650490\cdot10^{-3} - 6.202263\cdot10^{-4}\cdot e^{0.613913\cdot x}\right)\cdot\cos(0.306957\cdot x)\right.$$
$$\left. -(3.218247\cdot10^{-4} + 3.218247\cdot10^{-4}\cdot e^{0.613913\cdot x})\cdot\sin(0.306957\cdot x)\right) \qquad 0\le x\le 3\,m$$

$$w_2(x) = e^{-0.306957\cdot x}\cdot\left(\left(-5.454747\cdot10^{-3} - 5.727759\cdot10^{-4}\cdot e^{0.613913\cdot x}\right)\cdot\cos(0.306957\cdot x)\right.$$
$$\left. -(2.253137\cdot10^{-5} + 6.699410\cdot10^{-4}\cdot e^{0.613913\cdot x})\cdot\sin(0.306957\cdot x)\right) \qquad 3\le x\le 5\,m$$

$$w_3(x) = e^{-0.306957\cdot x}\cdot\left(\left(8.266908\cdot10^{-3} + 1.121122\cdot10^{-4}\cdot e^{0.613913\cdot x}\right)\cdot\cos(0.306957\cdot x)\right.$$
$$\left. -(1.476991\cdot10^{-2} + 3.268873\cdot10^{-5}\cdot e^{0.613913\cdot x})\cdot\sin(0.306957\cdot x)\right) \qquad 5\le x\le 8\,m$$

$$w_4(x) = e^{-0.306957\cdot x}\cdot\left(\left(7.586349\cdot10^{-3} + 1.623280\cdot10^{-4}\cdot e^{0.613913\cdot x}\right)\cdot\cos(0.306957\cdot x)\right.$$
$$\left. -(7.949772\cdot10^{-3} + 2.767785\cdot10^{-5}\cdot e^{0.613913\cdot x})\cdot\sin(0.306957\cdot x)\right) \qquad 8\le x\le 10\,m$$

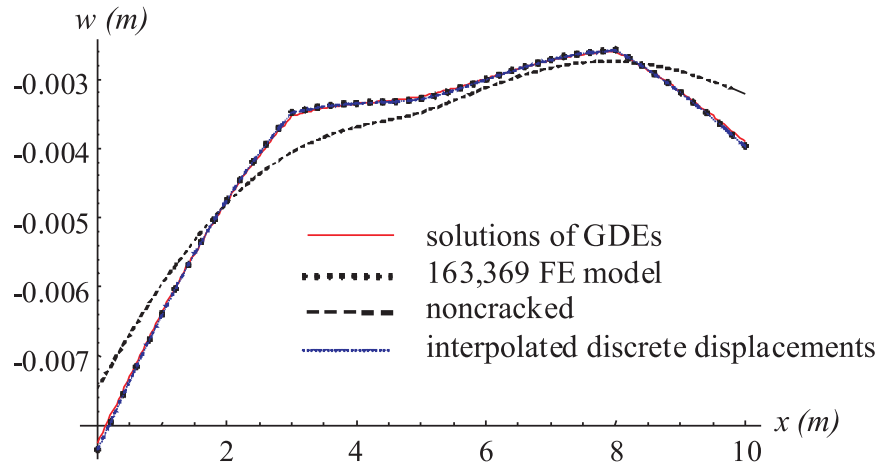

Figure 3. Comparison of transverse displacements.

The transverse displacements along the axis of the structure obtained by GDEs were compared to the discrete values obtained from the FE mesh, and are presented in Fig. 3, where only small discrepancies are noticeable. The transverse displacements for the non-cracked structure are also shown, exclusively to emphasize the effect of the introduced cracks.

The stress distribution at the soil surface can be obtained directly by multiplying the transverse displacements by the constant of proportionality. Fig. 4, therefore, shows the complete beam in the deformed state with the distance between the nodes being approximately 1 cm. It is obvious from Fig. 4 that the deformed curve of the contact surface is smooth and without any significant variations.

The same behaviour is evident, even in the vicinities of both cracks, Fig. 5 and, consequently, it can be concluded that strong local variations of the soil stresses are not actually presented.

It is further evident from Fig. 5 that open cracks do not exhibit any unexpected behaviour.

The differences between the displacements from both models were additionally examined since the transverse displacements represent a foundation for a further analysis of the inner forces and the bending moments. Fig. 6 shows the discrepancies in the results from both computational models at some discrete points along the structure. As expected, slightly larger discrepancies appeared at all the positions of the local effects (applied transverse loads and cracks). The average discrepancy was slightly below 0.77 %, with a maximum positive discrepancy of 2.01 % appearing at the right-end, and a maximum negative discrepancy of 2.09 % appearing at the left crack. It should be mentioned that the non-cracked situation was also considered, bringing the average discrepancy slightly below 0.37 %, with a maximum discrepancy of 1.19 % appearing at the mid-span. This proves that the discrepancies for the cracked situation do not originate solely from the applied simplified model.

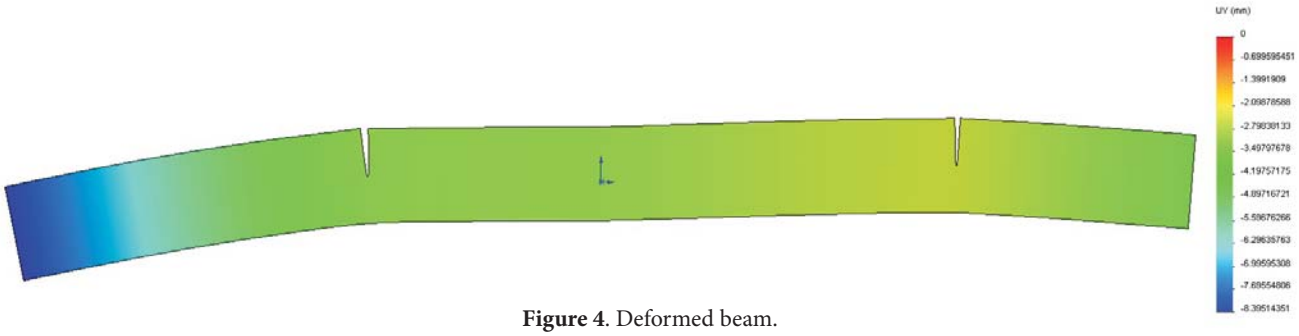

Figure 4. Deformed beam.

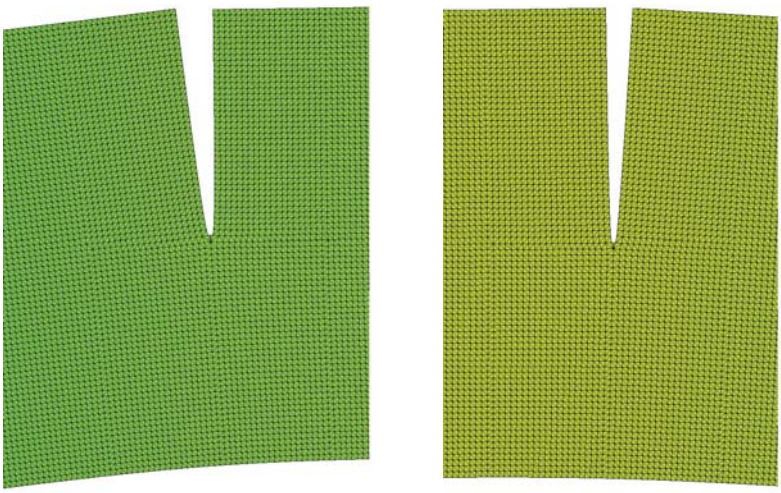

Figure 5. Details of the beam deformed state in the vicinity of the cracks.

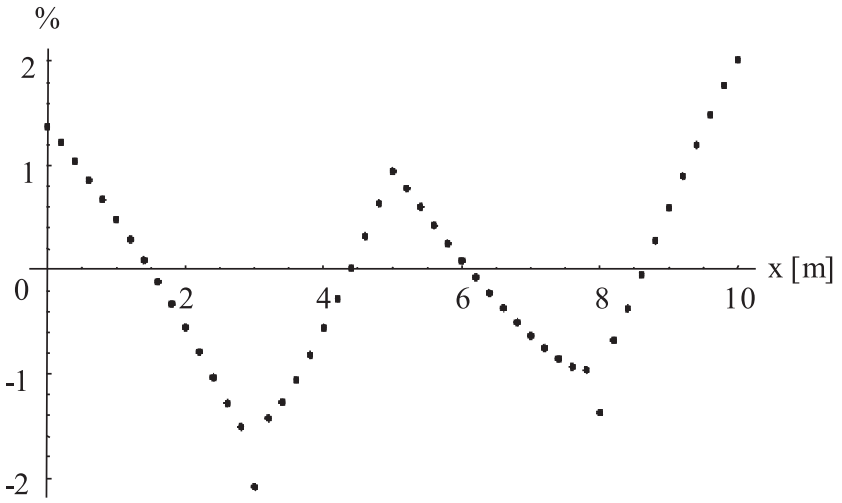

Figure 6. Discrepancies in transverse displacements.

Afterwards, the solution of GDEs allowed the bending moments to be evaluated analytically along the structure by implementing the second derivatives of the transverse displacement functions. The results obtained with this approach coincide completely at every point with the values obtained from the simple equilibrium conditions of the rotations.

Furthermore, the bending moment values from the 2D FE model were additionally required in order to provide a reliable assesment of the obtained results. Two unrelated approaches were conducted, since the bending moment values could not be retrieved directly from the 2D FE computational model. In the first approach, polynomial interpolation was utilized individually for all four regions in order to construct transverse displacement functions within the range of each discrete set of evaluated displacements (presented in Fig. 3). When using a polynomial interpolation, the interpolant is a polynomial and, thus, infinitely differentiable, which then made it possible to determine the bending-moment functions. However, although the matching of the transverse displacement functions was excellent and completely without any oscillatory artefacts, these negative effects become more than just evident at the end points of all four bending-moment functions, Fig. 7 (dashed line). Consequently, the interpolated transverse displacement functions were exclusively implemented within the equilibrium conditions of the rotations, thus providing results (dotted line) in excellent agreement with GDEs solutions from the simplified computational model (solid line).

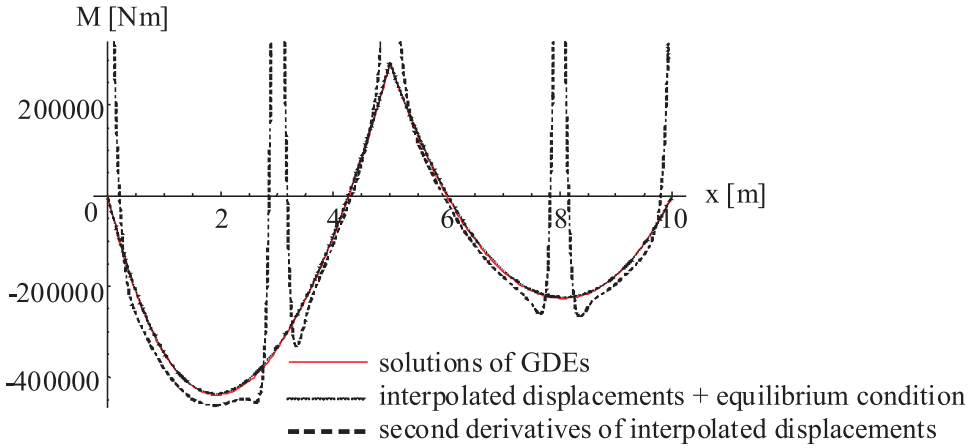

Figure 7. Comparison of bending moments.

In the second approach, the moments of normal stresses from the 2D FE model were numerically integrated in several selected transverse sections in order to construct bending moments. This approach produced values that were completely independent of the obtained displacements. Special attention was paid to those locations where the local stress singularities were caused by the applied concentrated loads or cracks, primarily due the fact that the stresses were actually obtained in Gauss integration points within the finite elements, and their nodal values were further obtained by extrapolation, automatically executed by the original algorithm of the FE software. Nevertheless, an excellent agreement of the results from both computational models was clearly proved when comparing the integrated values (discrete dots in Fig. 8) to the values obtained from the GDEs (solid line). The discrepancy in the results at the position of the maximum negative (hogging) moment (located between the left end and left crack) was 0.98 %, while at the position of maximum positive (sagging) moment (located at the mid-span), the discrepancy was 1.51 %. The discrepancies at the cracks' locations were 1.71 % and 1.17 % for the left- and right-hand cracks, respectively.

An identical situation was also detected when the shear forces were studied and all four computational techniques were implemented. Again, both computations based on GDEs solutions of the simplified model (the third derivative of transverse displacements, as well as the applied vertical equilibrium) produced identical results (red solid line in Fig. 9). Furthermore, the first solution based on the discrete displacements from the FE model, i.e., the implementation of the interpolated displacements within the condition of the vertical equilibrium, again provided an exceptional agreement with the first two approaches (dashed line). Like with the bending moments, the integration of the shear stresses from the FE model at certain selected cross-sections (discrete dots) again produced excellent matching of the results, even at the centre of the structure, where a concentrated transverse load was applied and, consequently, an abrupt change in the shear forces was expected.

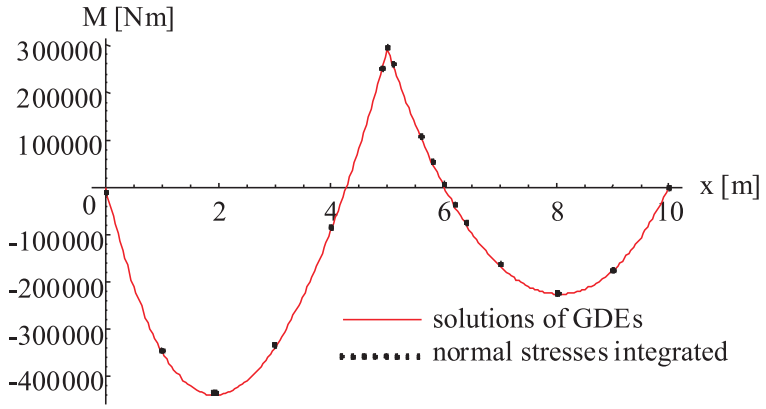

Figure 8. Comparison of bending moments.

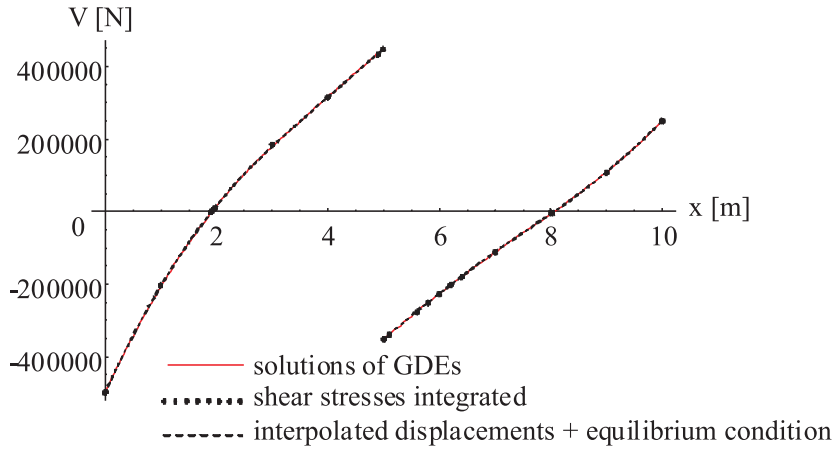

Figure 9. Comparison of shear forces.

The discrepancy of the results at the position of the maximum negative shear force (located at the left-end) was 0.12 %, while at the position of the maximum positive shear force (located at the left-hand side of the midspan) the discrepancy was 0.28 %.

3.3 LOAD CASE 2: THREE CONCENTRATED DOWNWARD FORCES AND TWO UNIFORM TRANSVERSE LOADS

In the second load case, three vertical downward transverse forces from the first load situation remained on the structure; however, both side forces were shifted by 20 cm towards the centre of the beam. Furthermore, two uniform transverse continuous loads were applied. The downward uniform load of 50 kN/m was applied in the region between the left-end and the mid-span of the structure, while the remainder of the element was loaded by a downward uniform load of 75 kN/m, Fig. 10.

3.4 LOAD CASE 2: RESULTS AND DISCUSSION

Since the structure had two cracks and three concentrated in-field transverse loads, the corresponding computational model of the considered load combination consisted of six elastic segments. Consequently, six coupled functions for six elastic regions had to be analyzed in order to obtain the vertical displacement distributions along the structure. Since the distributed load was applied to each part of the structure, the interpolation function for each region followed the mathematical form of Eq.(2), with the particular integral equal to *-q/k*.

The following functions for the transverse displacements were obtained from a system of coupled governing differential equations (GDEs) by the implementation of mechanical boundary conditions, as well as the continuity conditions:

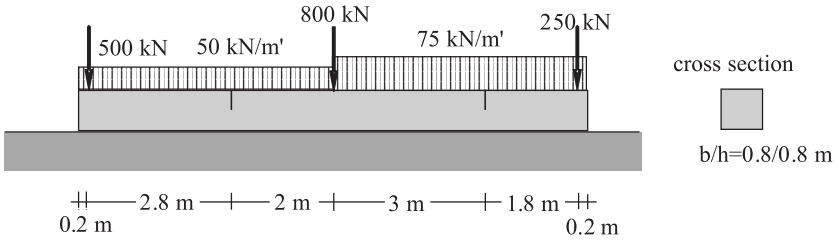

Figure 10. Second example setup.

$$w_1(x) = e^{-0.306957\cdot x}\cdot\left(-5.032285\cdot10^{-3}\cdot\cos(0.306957\cdot x) + 1.250409\cdot10^{-3}\cdot\sin(0.306957\cdot x)\right) - 1.25\cdot10^{-3}$$
$$+e^{0.306957\cdot x}\cdot\left(-2.531466\cdot10^{-3}\cdot\cos(0.306957\cdot x) + 1.250409\cdot10^{-3}\cdot\sin(0.306957\cdot x)\right) \qquad 0 \le x \le 0.2\ m$$

$$w_2(x) = e^{-0.306957\cdot x}\cdot\left(-6.943232\cdot10^{-3}\cdot\cos(0.306957\cdot x) - 9.108504\cdot10^{-4}\cdot\sin(0.306957\cdot x)\right) - 1.25\cdot10^{-3}$$
$$+e^{0.306957\cdot x}\cdot\left(-6.199267\cdot10^{-4}\cdot\cos(0.306957\cdot x) - 4.397391\cdot10^{-4}\cdot\sin(0.306957\cdot x)\right) \qquad 0.2 \le x \le 3\ m$$

$$w_3(x) = e^{-0.306957\cdot x}\cdot\left(-5.003725\cdot10^{-3}\cdot\cos(0.306957\cdot x) - 6.464836\cdot10^{-4}\cdot\sin(0.306957\cdot x)\right) - 1.25\cdot10^{-3}$$
$$+e^{0.306957\cdot x}\cdot\left(-5.780136\cdot10^{-4}\cdot\cos(0.306957\cdot x) - 7.472313\cdot10^{-4}\cdot\sin(0.306957\cdot x)\right) \qquad 3 \le x \le 5\ m$$

$$w_4(x) = e^{-0.306957\cdot x}\cdot\left(8.770142\cdot10^{-3}\cdot\cos(0.306957\cdot x) - 1.394470\cdot10^{-2}\cdot\sin(0.306957\cdot x)\right) - 1.875\cdot10^{-3}$$
$$+e^{0.306957\cdot x}\cdot\left(1.092993\cdot10^{-4}\cdot\cos(0.306957\cdot x) - 4.267824\cdot10^{-5}\cdot\sin(0.306957\cdot x)\right) \qquad 5 \le x \le 8\ m$$

$$w_5(x) = e^{-0.306957\cdot x}\cdot\left(8.213005\cdot10^{-3}\cdot\cos(0.306957\cdot x) - 8.361426\cdot10^{-3}\cdot\sin(0.306957\cdot x)\right) - 1.875\cdot10^{-3}$$
$$+e^{0.306957\cdot x}\cdot\left(1.504083\cdot10^{-4}\cdot\cos(0.306957\cdot x) - 3.857611\cdot10^{-5}\cdot\sin(0.306957\cdot x)\right) \qquad 8 \le x \le 9.8\ m$$

$$w_6(x) = e^{-0.306957\cdot x}\cdot\left(3.004931\cdot10^{-2}\cdot\cos(0.306957\cdot x) + 8.306926\cdot10^{-3}\cdot\sin(0.306957\cdot x)\right) - 1.875\cdot10^{-3}$$
$$+e^{0.306957\cdot x}\cdot\left(1.097615\cdot10^{-4}\cdot\cos(0.306957\cdot x) + 1.467303\cdot10^{-5}\cdot\sin(0.306957\cdot x)\right) \qquad 9.8 \le x \le 10\ m$$

The transverse displacements along the axis of the structure obtained by the GDEs were compared to the discrete values obtained from the FE mesh, as presented in Fig. 11, where only small discrepancies are noticeable. The transverse displacements for the non-cracked structure are also shown, exclusively to emphasize the effect of the introduced cracks.

The differences between the displacements from both models were further examined. Figure 12 shows the discrepancies in the results from both computational models at some discrete points along the structure. Again, extreme local discrepancies appeared at all positions regarding local effects (applied transverse loads and cracks). Compared to the first load case, the average discrepancy was even better, i.e., slightly below 0.5 %. Furthermore, both of the obtained extreme values were also lower. A maximum positive discrepancy of 1.18 % and a maximum negative discrepancy of 1.33 % again appeared at the same points: at the right-end and the left-crack, respectively. It should also be noted that, for the considered load case, the discrepancy at the right-crack also decreased, while at the left-end of the structure the discrepancy remained almost identical, when compared to the first load case.

The bending moments were evaluated analytically along the structure by implementing the second derivatives of the transverse displacement functions from the solutions of the GDEs. The results obtained with this approach at every point coincided completely with those values obtained from the simple equilibrium conditions of the rotations.

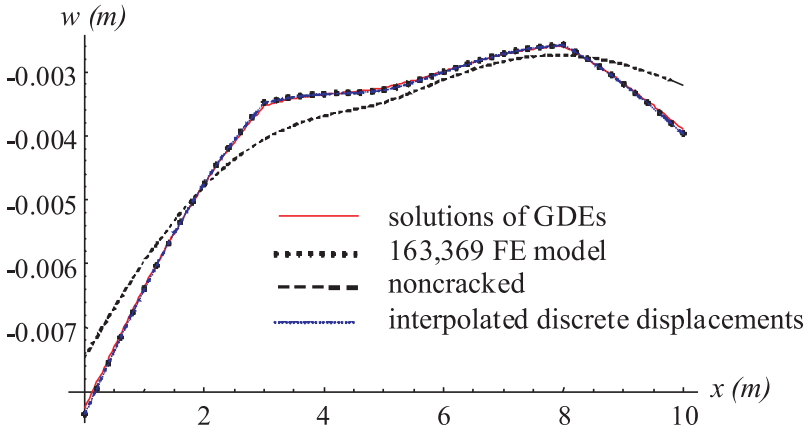

Figure 11. Comparison of transverse displacements.

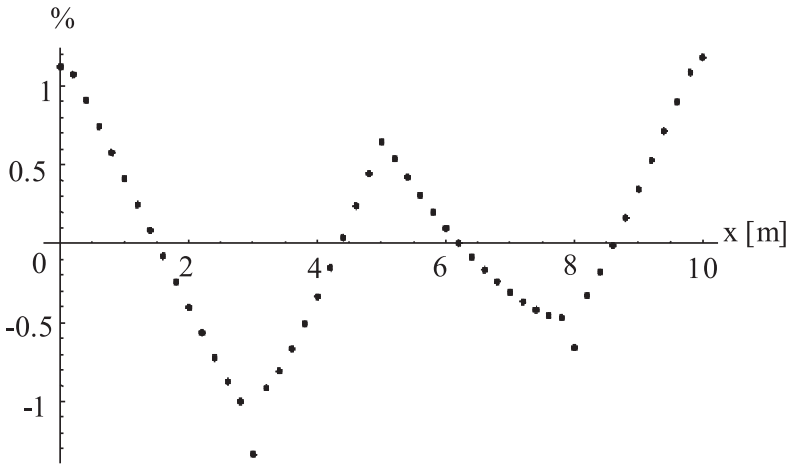

Figure 12. Discrepancies of transverse displacements.

As in the first load case, the displacement results from the 2D FE model were additionally implemented in two approaches for the comparative evaluation of the bending moments. In the first approach a polynomial interpolation was again utilized individually for all six regions in order to construct the transverse displacement functions within the range of each discrete set of evaluated displacements. However, it transpired that the transverse displacements for both short-ending regions can also be completely and adequately described by those functions belonging to the next neighbouring region. The interpolated functions were afterwards implemented within the equilibrium conditions of the rotations, providing results (dotted line) in excellent agreement with GDEs solutions from the simplified computational model (solid line), Fig. 13. In the second approach, the moments of the normal stresses from the discrete points of the FE model were numerically integrated within several selected transverse sections in order to construct the bending moments (discrete dots in Fig. 11), again proving the quality of the results from the simplified model.

The discrepancy in the results at the position of the maximum negative (hogging) moment (located between the left-end and left-crack) was 1.07 %, whilst at the position of the maximum positive (sagging) moment (located at the mid-span) the discrepancy was 1.21 %. The discrepancies at the crack locations were 1.69 % and 1.13 % for the left and right-cracks, respectively.

The shear forces were aditionally studied, implementing all four computational techniques. As expected, both computations based on the GDEs solutions of the simplified model (the third derivative of the transverse displacements, as well as the applied vertical equilibrium) produced identical results (red solid line in Fig. 14). Furthermore, the first solution based

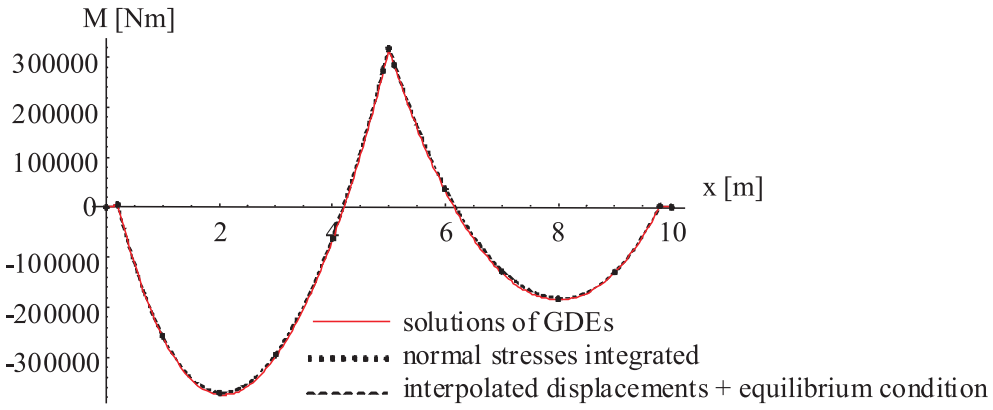

Figure 13. Comparison of bending moments.

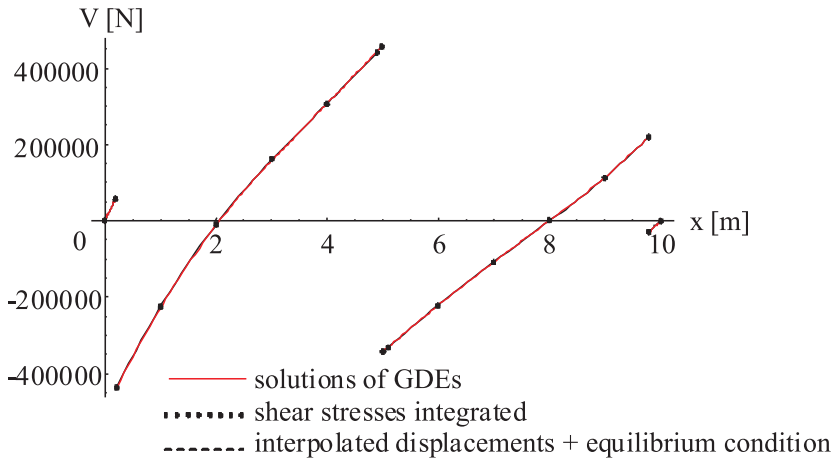

Figure 14. Comparison of shear forces.

on the discrete displacements from the FE model, i.e., the implementation of the interpolated displacements within the condition of the vertical equilibrium, again provided an exceptional agreement with the first two approaches (dashed line). Finally, the integration of the shear stresses at certain selected isolated cross-sections (discrete dots) again produced an excellent matching of the results, even within the positions of the concentrated transverse loads, where abrupt changes in the shear forces clearly appeared.

The discrepancy in the results at the position of the maximum negative shear force (located at the right-side of the left transverse force) was 1.59 %, while at the position of the maximum positive shear force (located at the left-side of the mid-span) the discrepancy was 0.30 %.

4 CONCLUSIONS

Okamura's simplified computational model of cracked beams was implemented to evaluate the transverse displacements and inner forces for transversely cracked slender beams resting on Winkler's foundation. The transverse displacements were firstly evaluated from solutions of coupled differential equations, while the implementation of well-known relationships from the Euler–Bernoulli beam theory further allowed for the bending moments and shear forces to be computed.

The results obtained with the discussed approach were afterwards compared to the results obtained from the pure numerical approach implementing parabolic triangular-shell finite elements within the framework of the finite-elements method. Despite the clear computational differences between both approaches, the considered examples showed that the application of the simplified model produces excellent matching results. The proposed computational model has also proved itself to be useable for beams on Winkler's foundation, as the discrepancies in the results obtained with this approach compared with the results obtained with much more complex and time-consuming 2D finite-elements models are just up to 2.2 %, despite the enormous differences in the computational effort. Furthermore, the transverse displacement solutions obtained from differential equations are given in analytical form, which allows for a straightforward further analysis of the bending moments and shear forces.

The proposed approach thus yields an adequate, as well as accurate, approach for the modelling of cracked beam structures in engineering situations where the cracks have to be considered during the analysis.

REFERENCES

[1] Okamura H., Liu H.W., Chorng-Shin C. (1969). A cracked column under compression, Eng. Frac. Mech. 1, 547-564.

[2] Ostachowicz W.M., Krawczuk M. (1990). Vibrational analysis of cracked beam, Comp. and Struc. 36-22, 245-250.

[3] Dimarogonas A.D., Papadopulus C.A. (1983). Vibration of cracked shafts in bending. J. Sound Vib. 91(4), 583-593.

[4] Rajab M.D., Al-Sabeeh A. (1991). Vibrational characteristics of cracked shafts, J. Sound and Vib. 147(3), 465-473.

[5] Krawczuk M., Ostachowicz W.M. (1993). Influence of a crack on the dynamic stability of a column, J Sound Vib. 167(3), 541-555.

[6] Sundermayer J.N., Weaver R.L. (1993). On crack identification and characterization in a beam by nonlinear vibration analysis, Theoretical and applied mechanics, TAM Report No. 743, UILU-ENG-93-6041.

[7] Hasan W.M. (1995). Crack detection from the variation of the eigenfrequencies of a beam on elastic foundation, Eng. Frac. Mec. 52(3), 409-421.

[8] Skrinar M., Pliberšek T. (2004). New linear spring stiffness definition for displacement analysis of cracked beam elements, Proc. Applied. Math. Mechanics 4, 654-655.

[9] Shifrin E.I., Ruotolo R. (1999). Natural frequencies of a beam with an arbitrary number of cracks, J. Sound Vib. 222, 409-423.

[10] Khiem N.T., Lien T.V. (2001). A simplified method for natural frequency analysis of a multiple cracked beam, J. Sound Vib. 245, 737-751.

[11] Li Q.S. (2002). Free vibration analysis of non-uniform beams with an arbitrary number of cracks and concentrated masses, J. of Sound Vib., 252, 509-525.

[12] Fernández-Sáez J., Navarro C. (2002). Fundamental frequency of cracked beams in bending vibrations: an analytical approach, J. Sound and Vib. 256(1), 17-31.

[13] Rizos P.F., Aspraghtas N., Dimarogonas A.D. (1990). Identification of crack location and magnitude in a cantilever beam from the vibration modes, J. Sound Vib. 138, 381-388.

[14] Boltežar M., Štrancar B., Kuhelj A. (1998). Identification of transverse crack location in flexural vibrations of free-free beams, J. Sound Vib. 211(5), 729-734.

[15] Vestroni F., Capecchi D. (2000). Damage detection in beam structures based on frequency measurements, J. Eng. Mech. 126, 761-768.

[16] Bamnios Y., Douka E., Trochidis A. (2002). Crack identification in beam structures using mechanical impedance, J. Sound Vib. 256(2), 287-297.
[17] Gounaris G., Dimarogonas A.D. (1988), A finite element of a cracked prismatic beam for structural analysis, Comp. Struc. 28(3), 301-313.
[18] Skrinar M., Umek A. (1996). Plane beam finite element with crack, J. Gradbeni vestnik (in Slovenian)1&2, 2-7.
[19] Skrinar M. (2007). On the application of a simple computational model for slender transversely cracked beams in buckling problems, Comput. mater. sci. 39(1), 242-249.
[20] Krawczuk M., Žak A., Ostachowicz W. (2000). Elastic beam finite element with a transverse elasto-plastic crack, Finite Elem. Anal. Design 34, 61-73.
[21] Kisa M., Brandon J. (2000). The effects of closure of cracks on the dynamics of a cracked cantilever beam, J. Sound Vib. 238(1), 1-18.
[22] Skrinar M. (2009). Elastic beam finite element with an arbitrary number of transverse cracks, Finite Elem. Anal. Des. 45(3), 181-189.
[23] Caddemi S., Caliò I. (2008). Exact solution of the multi-cracked Euler-Bernoulli column, International J. of Solids and Structures 45 (16), 1332-1351.
[24] Biondi B., Caddemi S. (2007). Euler-Bernoulli beams with multiple singularities in the flexural stiffness, European J. Mechanics A/Solids 26 (5), 789-809.
[25] Biondi B., Caddemi S. (2005). Closed form solutions of Euler–Bernoulli beams with singularities, J. of Solids and Structures 42, 3027–3044.
[26] Jones G. (1997). Analysis of beams on elastic foundations: using finite difference theory, Thomas Telford.
[27] Chen C. N. (1998). Solution of beam on elastic foundation by DQUM. Journal of Engineering Mechanics, December, 1381-1384.
[28] Onu G. (2000). Shear effect in beam finite element on two- parameter elastic foundation. Journal of Engineering Mechanics, September, 1104-1107.
[29] Guo Y. J. and Weitsman Y. J. (2002). Solution method for beams on nonuniform elastic foundations. Journal of Engineering Mechanics, American Society of Civil Engineers, 128, No. 5, May, 592-594.
[30] Al- Azzawi A. A., Mahdy A. H., Farhan O. Sh. (2010), Finite element analysis of deep beams on nonlinear elastic foundations, Journal of the Serbian Society for Computational Mechanics, Vol. 4 , No. 2, 13-42.
[31] Cerioni R., Mingardi L. (1996). Nonlinear analysis of reinforced concrete foundation plates, Computers & Structures, 61, 1, 87-106.
[32] Melerski E. S. (2000). Design Analysis of Beams, Cicular Plates and Cylindrical Tanks on Elastic Foundations: With IBM Compatible Software – Hardcover, Balkema, A. A. Publishers.
[33] Oden J. T. (1967). Mechanics of elastic structures, New York: McGraw-Hill.
[34] Selvadurai A.P.S. (1979). Elastic analysis of soil-foundation interaction, Elsevier Scientific Pub. Co., Amsterdam.
[35] Vestroni F. (2009). Lecture notes from the course Dynamical Inverse Problems: Theory and Application, Udine.